JOURNAL OF
AGRICULTURAL AND
FOOD CHEMISTRY
ARTICLE

Influence of Reducing Carbohydrates on (6*S*)-5-Methyltetrahydrofolic Acid Degradation during Thermal Treatments

PHILIPPE H. C. J. VERLINDE,[†] INDRAWATI OEY,[‡] LIEN LEMMENS,[†]
WIM M. DEBORGGRAEVE,[§] MARC E. HENDRICKX,[†] AND ANN M. VAN LOEY*[,†]

[†]Laboratory of Food Technology and Leuven Food Science and Nutrition Research Centre (LFoRCe), Department of Microbial and Molecular Systems (M2S), Katholieke Universiteit Leuven, Kasteelpark Arenberg 22, Box 2457, 3001 Leuven, Belgium, [‡]Department of Food Science, University of Otago, 276 Leith Walk, P.O. Box 56, Dunedin 9054, New Zealand, and [§]Division of Molecular Design and Synthesis, Department of Chemistry, Katholieke Universiteit Leuven, Celestijnenlaan 200F, Box 2404, B-3001 Leuven, Belgium

The mechanism and kinetics of the degradation of (6*S*)5-methyl-5,6,7,8-tetrahydrofolic acid in an aqueous solution in the presence of reducing carbohydrates such as glucose and fructose were investigated for thermal treatments. Preliminary experiments indicated that the presence of reducing carbohydrates, especially fructose (1.6 mM–1.5 M), strongly enhanced folate degradation at moderate temperatures (50–90 °C, 0–60 min). Identification of the predominant folate degradation products by LC-MS and NMR pointed to the formation of $N(2\alpha)$-[1-(carboxyethyl)]-5-methyl-5,6,7,8-tetrahydrofolic acid diastereomers besides other folate degradation products upon prolonged heating (24 h, 100 °C) of (6*S*)5-methyl-5,6,7,8-tetrahydrofolic acid in fructose or dihydroxyacetone solutions. Using a Bayesian multiresponse kinetic modeling approach, kinetic characterization and elucidation of the degradation mechanism in the presence of equimolar amounts of dihydroxyacetone, fructose, and glucose were achieved. On the basis of the established degradation mechanism for (6*S*)5-methyl-5,6,7,8-tetrahydrofolic acid oxidation in the literature, it was shown that nonenzymatic glycation occurred due to reaction of dihydroxyacetone with 5-methyl-7,8-dihydrofolic acid. During thermal treatments (85–110 °C, 0–60 min), the nonenzymatic glycation reaction was characterized by an activation energy of 61.3 ± 9.3 and 77.6 ± 7.8 kJ mol^{-1} in the presence of, respectively, dihydroxyacetone and fructose. Addition of L-ascorbic acid (1.13 mM) to folate samples (0.04 mM) with equimolar amounts of fructose prior to heating (100 °C, 0–45 min) was shown to retard the formation of 5-methyl-7,8-dihydrofolic acid and hence prevented the formation of the carboxyethylated derivatives under the investigated conditions.

KEYWORDS: Nutrient degradation; folate; carboxyethylated folate; multiresponse modeling; Maillard reaction; nonenzymatic glycation; temperature; kinetics

INTRODUCTION

Tetrahydrofolic acid and its derivatives, collectively termed folates (vitamin B$_{11}$), are essential cofactors in human metabolism, playing a key role in one-carbon transfer reactions in biosynthetic and epigenetic processes. Folates cannot be synthesized *de novo* by man and are present in pro- and eukaryotic cells as a class of structurally related pteridine derivatives, composed of 2-amino-4-hydroxypteridine bound through a methylene carbon to *p*-aminobenzoyl-L-glutamic acid or its γ-linked poly-L-glutamate derivatives. Over the past decades, adequate folate intake has been recognized as an important health-promoting factor due to the growing evidence pointing to the contribution of folate inefficiency to severe health disorders such as neural tube

defects (*1*), cardiovascular disease (*2*), neuropsychiatric conditions (*3*), and certain types of cancer (*4*).

An extensive number of studies have shown that folates can be subjected to enzymatic (*5*, *6*) and nonenzymatic reactions (*7*–*12*) during food processing, which thereby influence the amount of folates available for absorption during digestion of food. Although various folate vitamers have been shown to differ in sensitivity toward degradation, irreversible folate losses have generally been attributed to leaching and oxidative degradation, yielding biologically inactive pteridine derivatives and *p*-amino-benzoyl-L-glutamate (*13*, *14*). It has, however, been suggested that reactions of folates with other food components have to be considered in addition to oxidative degradation because the importance of a Maillard-like reaction involving reducing carbohydrates and the primary N(2) amine of folic acid has recently been reported (*15*, *16*). The aforementioned nonenzymatic glycation

*Corresponding author (telephone +32 16 321567; fax +32 16 321960; e-mail ann.vanloey@biw.kuleuven.be).

Article

J. Agric. Food Chem., Vol. 58, No. 10, 2010 **6191**

reaction, yielding $N(2\alpha)$-[1-(carboxy)ethyl]folic acid as predominant degradation product, has been shown to take place upon heating of aqueous and low-moisture (e.g., cookies) model systems containing folic acid in the occurrence of dihydroxyacetone or reducing carbohydrates as fructose, glucose, maltose, or lactose and accounted for 8−40% of the absolute loss of folic acid caused by the investigated thermal treatments (*15*, *16*).

In contrast to folic acid, the fully oxidized synthetic folate form, natural folates occur as 5,6,7,8-tetrahydropteridines that are more prone to oxidative degradation. To date, however, knowledge of the occurrence or relevance of nonenzymatic glycation reactions in the degradation of tetrahydrofolates is lacking. Therefore, the main objective of this research was to investigate the degradation mechanism of one of the predominantly occurring natural folate derivatives from plant-based foods, that is, (6*S*)5-methyl-5,6,7,8-tetrahydrofolic acid (5-MTHF, **1**) (*17*), in the occurrence of reducing carbohydrates and their degradation products using the oxidative degradation mechanism of 5-MTHF that was recently reported (*12*). To assess the impact of reducing carbohydrates on the degradation of 5-MTHF, single-response modeling was used as a starting point to qualitatively characterize the impact of reducing carbohydrates such as glucose and fructose. Second, the predominant nonenzymatic glycation products were purified and identified to enable quantification of these components. This knowledge was subsequently used to postulate a candidate reaction model for the degradation mechanism at atmospheric pressure in the presence of dihydroxyacetone by using a multiresponse kinetic modeling approach. Once the degradation mechanism was established, the concomitant kinetic reaction model was applied to investigate the impact of fructose, glucose, and L-ascorbic acid on the thermal degradation of 5-MTHF.

MATERIALS AND METHODS

Materials. All chemicals and reagents used were of analytical or HPLC grade purity. (6*S*)5-Methyl-5,6,7,8-tetrahydrofolic acid ((6S)5-MTHF) was donated as calcium salt by Eprova AG (Schaffhausen, Switzerland). 5-Methyl-7,8-dihydrofolic acid (5-MDHF, **2**) and *p*-aminobenzoyl-L-glutamic acid (p-ABG, **3**) were purchased from Schircks Laboratories (Jona, Switzerland) and stored in ampules under argon atmosphere at −80 °C. The predominant oxidative degradation product from 5-MTHF, that is, 2-amino-8-methyl-4,9-dioxo-7-methyl-*p*-aminobenzoylglutamate-6,7,8,9-tetrahydro-4*H*-pyrazino(1,2-a)-s-triazine (**4**), was obtained as previously described (*12*). All solutions were prepared using reagent-grade water (18 MΩ, 25 °C, Simplicity Water Purification System, Millipore, Molsheim, France).

Samples and Treatments. Samples of 5-MTHF (0.2−200 μg/mL, ≈0.4−400 μM) were freshly dissolved in water with various concentrations of dihydroxyacetone, fructose, or glucose (0−1.5 M) for each experiment. To standardize the initial oxygen content to 228−258 μM, all solutions were thermostated at 25 °C and flushed with humidified air (0.35 L min⁻¹, 20 min, 25 °C). Samples were filled in glass vials (800 μL, 8.2 × 30 mm, Cleanpack, Belgium) and capped with precaution taken to avoid the inclusion of air bubbles. For subsequent thermal treatments at 50−90 °C, samples were immersed in a water bath during preset time intervals of 0−60 min, whereas silicone oil (M1028/50, Roger Coulon, Brussels, Belgium) was used as heating medium for multiresponse kinetic experiments at 85−110 °C. After thermal treatments, samples were immediately immersed in ice water (0−4 °C) and stored for a maximum of 15 min to minimize further degradation reactions prior to HPLC analysis.

Chromatographic Methods. Analytical, LC-MS, and semipreparative chromatography of folates and related compounds was performed using the equipment and methodologies previously described (*12*). Quantitative analysis of 5-MTHF, its oxidative degradation, and its glycation products was performed using a 1200 series chromatograph (Agilent Technologies, Diegem, Belgium) equipped with a 1200 series UV-DAD detector. Chromatographic separation was achieved at 25 °C using an analytical Zorbax XDBC18 column (150 × 4.6 mm, 5 μm particle size, Agilent Technologies) with aqueous 0.1% formic acid (solvent A) and methanol (solvent B) as eluents. Prior to injection (20 μL), the column was equilibrated with 1 column volume (CV) of 12% methanol (v/v, A:B) at a flow rate of 0.5 mL min⁻¹. After injection, components were eluted for 1 CV using 12% methanol, followed by a linear gradient to 56% methanol (v/v, A:B) in 3 CVs. Subsequently, the column was washed with 56% methanol for 2 CVs. For quantification, detection was performed at 290 nm, whereas 2D spectra (220−400 nm) were continuously recorded to assess peak purity based on reference spectra obtained from external standards. Quantification of the different components (0−0.10 mM) was performed using external calibration curves based on peak area at 290 nm.

Analysis of glucose and fructose (0−0.08 mM) was performed using a high-performance anion-exchange chromatograph (Dionex, Sunnyvale, CA) equipped with a pulsed amperometric detector (ED50 detector, Dionex). For carbohydrate detection a quadrupole potential waveform (0.00 s, 0.1 V; 0.40 s, 0.1 V; 0.41 s, −2.0 V; 0.42 s, −2.0 V; 0.43 s, 0.6 V; 0.44 s, −0.1 V; 0.50 s, −0.1 V) was used, whereas separation was performed at 30 °C using an analytical polymeric CarboPac PA1 column (250 × 4.0 mm, Dionex) with corresponding guard column (50 × 4.0 mm). Carbohydrates were eluted isocratically using 150 mM sodium hydroxide at a flow rate of 1 mL min⁻¹ for 10 min. Subsequently, the column was regenerated for 10 min using 200 mM sodium hydroxide. Quantification was performed on the basis of external calibration curves using lactose, added as internal standard to a concentration of 0.08 mM in all samples prior to injection (10 μL).

**Purification and Identification Methods.** For synthesis of nonenzymatic glycation products, 5-MTHF (≈2 mM) was incubated with 8 mM dihydroxyacetone or fructose in a closed vessel for 24 h at 100 °C and regularly shaken. During subsequent semipreparative chromatography, fractionation was performed on the basis of the absorbance signal at 290 nm. Purification was achieved by upscaling the analytical HPLC method to a semipreparative method using a Prevail RP C₁₈ column (250 × 10 mm, 5 μm particle size, Grace) on an ÄKTA purifier chromatograph (GE Healthcare). The injection volume was 500 μL and the flow rate 5.0 mL min⁻¹. Peaks with retention times at, respectively, 18.27 (fraction 1) and 20.14 min (fraction 2) were separately collected and pooled from 11 runs. Upon collection, fractions were frozen using liquid nitrogen and stored at −80 °C. Finally, the two fractions were lyophilized for 24 h, and the purified components were stored in capped vials under nitrogen atmosphere in a desiccator containing P₂O₅. To control the purity of the fractions, 0.11 and 0.24 mg of fractions 1 and 2, respectively, were dissolved in 1 mL of water, and each sample was subjected to analysis by HPLC-MS and UV-DAD and compared with the DAD and MS spectra obtained for the nonpurified sample (retention times and spectra were unchanged). For LC-MS analysis, the analytical HPLC method described above for quantification of 5-MTHF, its oxidative degradation, and glycation products, was applied on an 1100 series chromatograph (Agilent Technologies) equipped with an LCQ Advantage Ion Trap mass spectrometer (Thermo Electron Co., Boston, MA). The spectrometer was operated in full scan mode (m/e 100−1300) using positive electrospray ionization (ESI) with spray and capillary voltages of +5.5 kV and 24.4 V, respectively. The capillary temperature was 200 °C using nitrogen as sheath gas (80 mL min⁻¹). For MS/MS experiments, the capillary temperature was raised to 375 °C, and components (precursor ion ± 1 m/e) were subjected to a collision-induced dissociation (CID) source energy of 35%.

To avoid photodegradation, all samples were wrapped in aluminum foil during storage. Spectral identification of components at room temperature was performed in 500 μL of ²H₆-DMSO using a Bruker Avance 600 MHz spectrometer with a 5 mm probe (Bruker Belgium, Brussels, Belgium). For 1D ¹H measurements the procedure and acquisition parameters were as follows: number of scans (NS) = 128, time domain (TD) = 65536, size of real spectrum (SI) = 32768, spectral resolution (HZpPT) = 0.16 Hz. For DEPT135 measurements these parameters were NS = 32768, TD = 10240, SI = 16384, and HZpPT = 2.20 Hz. Those for COSY measurements were NS = 32, TD = 128 (F1), 2048 (F2), SI = 1024, and HZpPT = 7.0 Hz (F1 and F2); for HSQC measurements, NS = 256, TD = 256 (F1), 1024 (F2), SI = 1024, HZpPT = 24.41 Hz (F1), and 6.45 Hz (F2); for HMBC measurements, NS = 512 TD = 128 (F1), 4096 (F2), SI = 1024

(F1), 2048 (F2), and HZpPT = 32.77 Hz (F1), 3.22 Hz (F2); and for TOCSY measurements, NS = 16, TD = 256 (F1), 2048 (F2), SI = 1024 (F1 and F2), and HZpPT = 5.98 Hz (F1 and F2).

The two purified degradation products exhibited very similar ^{1}H NMR and ^{13}C NMR spectral characteristic for $N(2\alpha)$-[1-(carboxy)ethyl)]-5-methyl-5,6,7,8-tetrahydrofolic acid (2-CE-5-MTHF, **6**, **Figure 1**). For fraction 1: ^{1}H NMR (^{2}H$_{6}$-DMSO COSY) δ 1.32 [3H, d, H$_{3}$-C(2γ'), J = 7.1 Hz], 1.90−1.96 [1H, m, H−C(19β)], 2.00−2.05 [1H, m, H−C-(19β)], 2.32 [2H, m, H$_{2}$-C(19α)], 2.50 [3H, s, H$_{3}$-C(5α)], 2.77−2.81 [1H, m, H$_{2}$-C(9)], 2.83−2.87 [1H, m, H$_{2}$-C(9)], 2.92−2.94 [1H, m, H−C(6)], 3.16 [2H, m, H$_{2}$-C(7)], 4.26−4.31 [1H, q, H−C(2β), J = 7.1 Hz], 4.32−4.36 [1H, q, H−C(19), J = 7.4 Hz], 6.05 [1H, t, H−N(10)], 6.25 [1H, d, H−N(2α), J = 7.4 Hz], 6.55 [2H, d, H−C(12) H−C(14), J = 8.5 Hz], 7.65 [2H, d, H−C(13) H−C(15), J = 8.7 Hz], 8.08 [1H, d, H−N(18), J = 7.3 Hz], 9.91 [1H, s, H−N(3)]; ^{13}C NMR (^{2}H$_{6}$-DMSO HSQC, HMBC, DEPT135) δ 18.68 [C(2γ')], 26.61 [C(19α)], 31.14 [C(19β)], 35.83 [C(7)], 42.95 [C(5α)], 43.92 [C(9)], 49.13 [C(2β)], 52.17 [C(19)], 55.57 [C(6)], 100.16 [C(4a)], 111.06 [C(12), C(14)], 120.79 [C(16)], 129.35 [C(13), C(15)], 151.63 [C(11)], 166.62 [C(17)], 174.00 [C(19γ)], 174.22 [C(19α')], 175.30 [C(2γ)]; ESI-MS [M + H] (positive ion mode) m/e 532; purity 86.0% (relative area at 290 nm upon HPLC analysis).

For fraction 2: ^{1}H NMR (^{2}H$_{6}$-DMSO COSY) δ 1.31 [3H, d, H$_{3}$−C-(2γ'), J = 7.1 Hz], 1.90−1.96 [1H, m, H−C(19β)], 2.00−2.05 [1H, m, H−C(19β)], 2.30 [2H, m, H$_{2}$-C(19α)], 2.49 [3H, s, H$_{3}$-C(5α)], 2.77−2.81 [1H, m, H$_{2}$-C(9)], 2.83−2.87 [1H, m, H$_{2}$-C(9)], 2.92−2.94 [1H, m, H−C(6)], 3.14 [2H, m, H$_{2}$-C(7)], 4.26−4.31 [1H, q, H−C(2β), J = 7.1 Hz], 4.32−4.36 [1H, q, H−C(19), J = 7.4 Hz], 6.05 [1H, t, H−N(10)], 6.25 [1H, d, H−N(2α), J = 7.4 Hz], 6.54 [2H, d, H−C(12) H−C(14), J = 8.5 Hz], 7.63 [2H, d, H−C(13) H−C(15), J = 8.7 Hz], 8.08 [1H, d, H−N(18), J = 7.3 Hz], 9.91 [1H, s, H−N(3)]; ^{13}C NMR (^{2}H$_{6}$-DMSO HSQC, HMBC, DEPT135) δ 18.52 [C(2γ')], 26.61 [C(19α)], 30.98 [C(19β)], 35.83 [C(7)], 43.11 [C(5α)], 43.92 [C(9)], 48.91 [C(2β)], 52.17 [C(19)], 55.57 [C(6)], 100.38 [C(4a)], 111.23 [C(12), C(14)], 121.01 [C(16)], 129.05 [C(13), C(15)], 151.85 [C(11)], 166.62 [C(17)], 172.48 [C(19γ)], 174.22 [C(19α')], 174.87 [C(2γ)]; ESI-MS [M + H] (positive ion mode) m/e 532; purity 82.0% (relative area at 290 nm upon HPLC analysis). Both components exhibited a λ_{max} at 287 ± 1 nm with ε 2.85 × 10^{3} cm^{-1} mol^{-1} L in
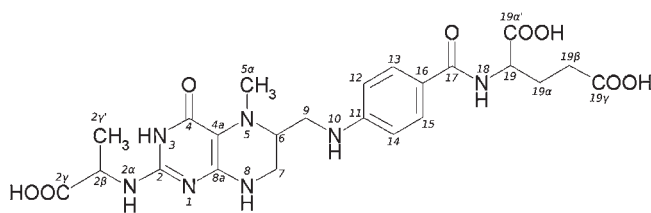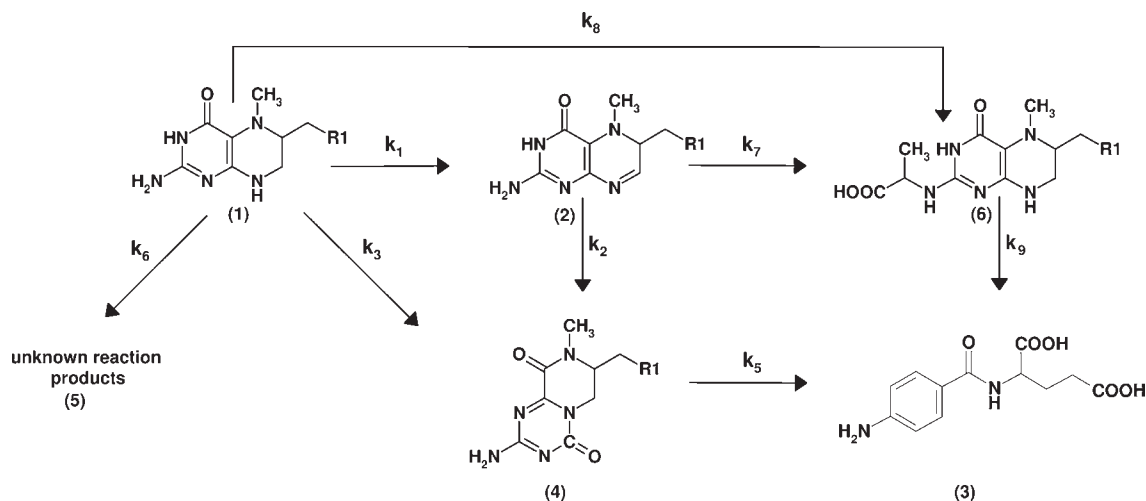
phosphate buffer (0.1 M, pH 7.0) and ε 2.79 × 10^{3} cm^{-1} mol^{-1} L in citrate buffer (0.1 M, pH 4.0).

Data Analysis. *Single Response Kinetic Modeling.* For single-response kinetic modeling, the temperature dependence of 5-MTHF degradation was approximated by an apparent first-order kinetic model using eq **1** and the Arrhenius equation (eq **2**), with C the concentration of 5-MTHF (mM) at time t (min), C_0 the initial concentration, E_a the activation energy (J mol^{-1}), R_g the universal gas constant (8.314 J mol^{-1} K^{-1}), and k_{Tref} the degradation rate constant (min^{-1}) at reference temperature T_{ref} (K). Parameters were estimated by simultaneously fitting both equations on the whole data set using nonlinear regression.

$$C = C_0\, e^{-kt} \tag{1}$$

$$k = k_{T_{ref}}\, e^{-E_a/R_g\left(\frac{1}{T}-\frac{1}{T_{ref}}\right)} \tag{2}$$

Multiresponse Kinetic Modeling. Multiresponse modeling was performed to investigate the degradation mechanism of 5-MTHF in the presence of reducing carbohydrates and their degradation products. On the basis of the identification of 2-CE-5-MTHF and the previously reported degradation mechanism for 5-MTHF in the absence of reducing carbohydrates (*12*), different reaction pathways were considered to characterize the formation of 2-CE-5-MTHF. Hereto, the aforementioned mechanism was revised to the mechanisms summarized in **Scheme 1**, with R1 representing the *p*-aminobenzoyl-L-glutamic acid part of the folate molecules.

In a multiresponse modeling approach, the measured responses were modeled simultaneously in an iterative process by the different reaction models. For each step in the reaction network, a differential equation was set up describing the reaction rate. For experiments with dihydroxyacetone, the nonenzymatic glycation reaction was represented as an apparent first-order reaction because concentrations of dihydroxyacetone could not be determined as response in the current study. For the most complex reaction network in **Scheme 1** this results in eqs **3**−**7**, where [**compound no.**] represents the concentration of the different compounds from **Scheme 1**, t represents the reaction time, and k represents the reaction rate constant with k_7 and k_8 accounting for the possible nonenzymatic glycation reactions.

$$\frac{d[\mathbf{1}]}{dt} = -(k_1 + k_3 + k_6 + k_7)[\mathbf{1}] \tag{3}$$

$$\frac{d[\mathbf{2}]}{dt} = k_1[1] - (k_2 + k_8)[\mathbf{2}] \tag{4}$$

$$\frac{d[\mathbf{3}]}{dt} = k_5[\mathbf{4}] + k_9[\mathbf{6}] \tag{5}$$

Figure 1. Atom numbering for $N(2\alpha)$-[1-(carboxy)ethyl)]-5-methyl-5,6,7,8-tetrahydrofolic acid.

Scheme 1

Table 1. Estimated k_{ref} (T_{ref} = 70 °C) and E_a Values for Degradation of 5-MTHF ($\approx$0.4 μM) in Water during Thermal Treatments (25–90 °C, 0–60 min) in the Presence of Fructose or Glucose[a]

	k_{ref} ($\times$ 10^{-3} min^{-1})	*P*	E_a (kJ mol^{-1})	*P*
control (0.4 μM 5-MTHF)	55.7 $\pm$ 8.57	<0.0001	88.2 $\pm$ 10.5	<0.0001
+ 1.6 mM D-fructose	118.4 $\pm$ 12.9	<0.0001	47.2 $\pm$ 7.7	<0.0001
+ 1.5 M D-fructose	101.8 $\pm$ 10.6	<0.0001	57.5 $\pm$ 5.4	<0.0001
+ 1.6 mM D-glucose	61.3 $\pm$ 5.57	<0.0001	86.8 $\pm$ 5.8	<0.0001
+ 1.5 M D-glucose	66.5 $\pm$ 4.38	<0.0001	63.7 $\pm$ 2.5	<0.0001

[a] Values are presented $\pm$ 95% HPD interval and parameter significance.
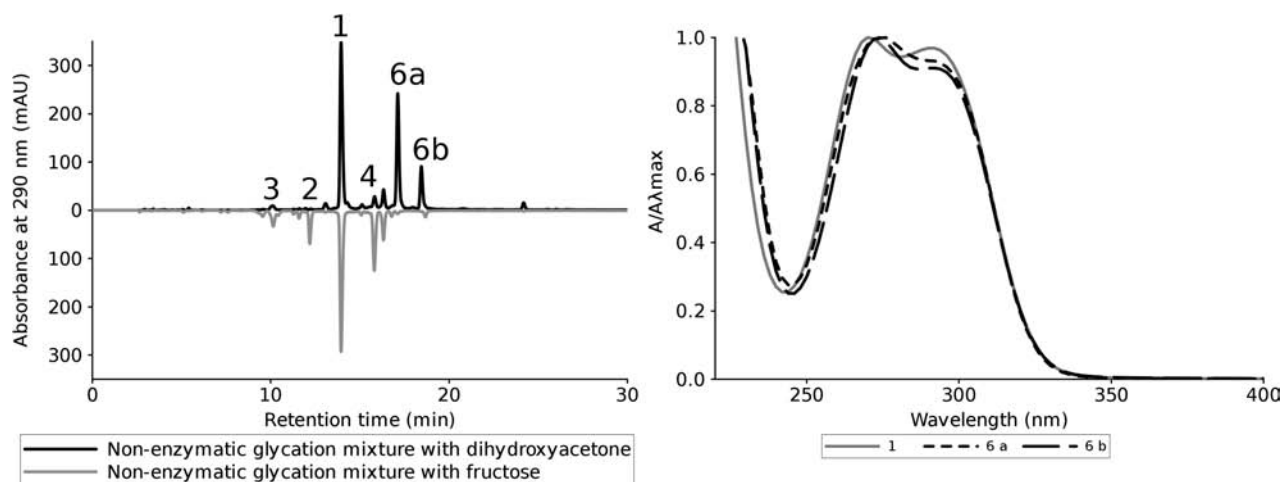
Figure 2. (Left) UV-DAD chromatograms of predominant degradation products of 5-MTHF (4 mM) formed in the presence of 16 mM dihydroxyacetone (top) or 16 mM fructose (bottom) after heating for 24 h at 100 °C. (Right) Overlay of UV-DAD spectra of 5-MTHF and its purified nonenzymatic glycation products.

$$\frac{d[\mathbf{4}]}{dt} = k_3[\mathbf{1}] + k_2[\mathbf{2}] - k_5[\mathbf{4}] \qquad (6)$$

$$\frac{d[\mathbf{6}]}{dt} = k_7[\mathbf{1}] + k_8[\mathbf{2}] - k_9[\mathbf{6}] \qquad (7)$$

The effect of temperature on each reaction was expressed by the Arrhenius equation (eq **2**), and substitution of this equation into the above differential equations rendered the mathematical model to be solved under isothermal conditions using numerical integration. The corresponding kinetic parameters, the reaction rate constants, and the activation energies of the various reactions were estimated simultaneously by nonlinear regression using the multiresponse Bayesian estimation software package Athena Visual Studio v12.1 (www.athenavisual.com). Conforming with the statistical demands for multiresponse modeling, the commonly used least-squares minimization was replaced by the determinant criterion as fit criterion (*18*). Model discrimination was based on the normalized marginal posterior probabilities for the candidate models and the lack of fit measure (*19*). Furthermore, the goodness of fit of the model was evaluated by scrutiny of the residuals, and the correlation matrix was inspected for abnormally high correlations between the different parameter estimates, that is, absolute values above 0.95. In addition, the performance of the different models was assessed in terms of other output statistics evaluating the quality of the model fit such as the objective function and the 95% confidence interval of the parameter estimates.

RESULTS AND DISCUSSION

Degradation during Thermal Treatments. In the first instance, the effect of excess amounts (1.6 mM–1.5 M) of fructose and glucose on the degradation of 5-MTHF ($\approx$0.4 μM) was investigated in water during thermal treatments (50–90 °C, 0–280 min). Under all investigated conditions, the degradation was adequately described with an apparent first-order kinetic model.

The estimated k_{ref} and E_a values, shown in **Table 1**, indicated that fructose concentrations of 1.6 mM and 1.5 M significantly enhanced the degradation rate of 5-MTHF (0.4 μM) and decreased the temperature dependence of the degradation rate constants because the latter resulted in significantly increased k_{ref} values and decreased E_a values. Increasing the concentration of fructose to 1.5 M did not result in significant differences in k_{ref} or E_a values. In the case of glucose, however, the activation energy was significantly decreased from 88.2 $\pm$ 10.5 kJ mol^{-1} for the control samples (0.4 μM 5-MTHF) to 63.7 $\pm$ 2.5 kJ mol^{-1} at 1.5 M glucose, whereas k_{ref} values did not significantly differ. Due to the low initial concentration of 5-MTHF, no nonenzymatic glycation or other degradation products were observed by fluorescence detection as they were probably below the detection limit of the current HPLC method. It was deemed necessary to identify the predominant degradation products formed in the presence of fructose or its degradation product dihydroxyacetone because the above results suggested that the observed acceleration of the degradation could be caused by the occurrence of a nonenzymatic glycation reaction in accordance with the literature (*15*, *16*).

Identification of Nonenzymatic Glycation Products. An aqueous solution of 5-MTHF ($\approx$2 mM) was heated (100 °C, 24 h) in the presence of 8 mM dihydroxyacetone or fructose and analyzed using the analytical HPLC method with UV-DAD and ESI-MS detection to identify the predominant degradation products. As shown in **Figure 2**, the thermal treatment resulted in the formation of two predominant components (**6a** and **6b**) in the presence of dihydroxyacetone. Both components were also observed in the chromatograms of the samples treated in the presence of fructose; however, compared to the known oxidation products of 5-MTHF, only minor amounts of these compounds were formed. A residual

peak of 5-MTHF was present in the chromatograms of the samples treated with dihydroxyacetone or fructose; however, this signal was remarkably lower in the samples with dihydroxyacetone compared to the signal in a reference "oxidation mixture", that is, 5-MTHF heated at 100 °C for 24 h in water. This observation suggested that 5-MTHF was less stable after consumption of the dissolved molecular O_2 (0.26 mM) in the presence of dihydroxyacetone and hence supported the role of the latter in an additional degradation pathway of 5-MTHF such as nonenzymatic glycation.

LC-MS analysis of the collected fractions after semipreparative chromatography yielded for both purified components **6a** and **6b** a protonated molecular ion with m/e 532.4 at the corresponding retention times that was characterized by the following CID fragmentation pattern (relative abundance): m/e 514.1 (6%), 417.1 (48%), 403.2 (16%), 399.1 (37%), 385.1 (100%), 367.2 (21%), 357.2 (6%). The three most intense fragmentation losses confirmed the addition of $\approx 72\,m/e$ units, probably a carboxyethyl moiety, in the pteridine part of 5-MTHF. Because also the UV−vis spectra of both purified components were almost identical (**Figure 2**), it can be suggested that the products are diastereomers of a carboxyethylated folate derivative in accordance with previous observations for folic acid in a similar reaction (*15*). Detailed clarification of the molecular structure of these components was performed on the basis of spectral analyses at 600 MHz in ^{2}H$_6$-DMSO. Both degradation products exhibited very similar ^{1}H NMR and ^{13}C NMR spectra characteristic for $N(2\alpha)$-[1-(carboxy)ethyl]-5-methyl-5,6,7,8-tetrahydrofolic acid (2-CE-5-MTHF, **6**). An overview of the assignments of carbon signals based on correlations in HSQC and HMBC measurements is shown in the Supporting Information. Comparison of the ^{1}H NMR spectra with the previously reported spectrum of 5-MTHF (*12, 20*) showed that all signals of the pteridine and *p*-aminobenzoyl-L-glutamic acid moiety were retained in both carboxyethylated derivatives, except for the characteristic singlet for $N(2\alpha)$-H$_2$ at 5.87 ppm that was shifted upfield to 6.25 ppm and split in a doublet, integrating for 1H. The concurrent rise of a $C(2\gamma')$ methyl signal as a doublet that correlated with the ^{13}C signals for $C(2\beta)$−H and $C(2\gamma)$−OOH in the HMBC spectra, plus the corresponding correlations between the relevant proton signals of H$_3$−C($2\gamma'$), H−C(2β), and H−N(2α) in TOCSY measurements, validated the covalent linkage of a carboxyethyl group on N(2α) and therefore the structure of 2-CE-5-MTHF. On the basis of the above measurements and in accordance with the oxidation mechanism for 5-MTHF (*12*), it could be suggested that the carboxyethylated degradation products originate either from 5-MTHF or from 5-MDHF during thermal treatments as described in **Scheme 1**.

Degradation Mechanism during Thermal Treatments. *Degradation in the Presence of Dihydroxyacetone.* Formation of carboxyethylated derivatives of folic acid as nonenzymatic glycation products of fructose has previously been reported to occur through a reaction with dihydroxyacetone (*15, 16*). A degradation mechanism based on the former observations (*15*) has been postulated; however, it should be noted that this mechanism has not yet been supported by a mechanistic study and hence remains tentative. To characterize the mechanism of nonenzymatic glycation of 5-MTHF in the presence of reducing carbohydrates, a multiresponse modeling approach was applied. Generally, the application of multiresponse modeling offers a good, but rarely used, way to elucidate reaction mechanisms and kinetics (*18*), especially in food science. Therefore, thermal experiments were performed to investigate the degradation of 5-MTHF (≈ 0.04 mM) in the presence of an equimolar amount of dihydroxyace-

tone. In comparison to the previous kinetic experiments in this study, a higher initial concentration of 5-MTHF (≈ 0.04 vs ≈ 0.4 μM) was chosen for the multiresponse experiments to ensure a measurable UV response of the carboxyethylated degradation products during HPLC analysis because these components exhibit a much lower absorbance characteristics ($\varepsilon \approx 2.8 \times 10^3$ cm^{-1} mol^{-1} L) compared to the other folate degradation products. In accordance with our previous work (*12*), concentrations of 5-MTHF, 5-MDHF, p-ABG, and the *s*-triazine oxidation products were quantifiable in thermally treated samples (85−110 °C, 0−60 min) with an initial O_2 concentration of 0.26 mM. It was observed that the concentration of 5-MTHF decreased with treatment time upon heating of the solutions, whereas concentrations of 5-MDHF and the *s*-triazine degradation product increased. Under all investigated conditions, a decrease in 5-MDHF and *s*-triazine coincided with detectable formation of p-ABG, whereas the rate of 5-MTHF degradation and the rate of formation of 5-MDHF and *s*-triazine increased with increasing treatment temperature. In addition to the aforementioned responses, low concentrations of 2-CE-5-MTHF were detected under the investigated conditions as depicted in **Figure 3**.

To model the degradation mechanism in the presence of dihydroxyacetone, kinetic models (**Scheme 1**) were constructed starting from the degradation mechanism of 5-MTHF (*12*) and the reaction mechanism postulated for the nonenzymatic glycation of folic acid (*15*). The formation of 2-CE-5-MTHF was hypothesized to occur by a nucleophilic attack of the exocyclic N(2α) amino group from 5-MTHF or 5-MDHF on dihydroxyacetone. Because the resulting component could possibly undergo C(9)−N(10) bond cleavage, a formation route for p-ABG from 2-CE-5-MTHF was considered in the tested reaction models. Hereto, the reaction models from **Scheme 1** were refined in an iterative procedure by simultaneously fitting different reaction models incorporating different possible formation routes of p-ABG and 2-CE-5-MTHF. Previously reported estimates for k_1−k_6 and the corresponding E_a values (*12*) were used as prior knowledge, that is, as starting values for estimation of the current parameters. On the basis of the normalized marginal posterior probability share of the different kinetic models, the candidate model described in **Scheme 2** resulted in the most accurate fit for the data, that is, values of 0.883 and 92.9 for the normalized marginal posterior probability and the lack of fit measure, respectively.

Scheme 2
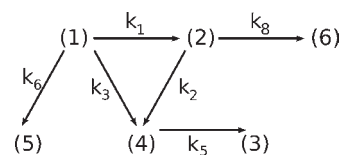
Predicted and experimental concentrations of the measured responses per temperature (85−110 °C) as a function of treatment time for 5-MTHF (**1**), 5-MDHF (**2**), p-ABG (**3**), and the *s*-triazine (**4**) are presented in **Figure 3**. Normal probability plots used to assess the model fit are presented in the Supporting Information. An accurate model fit was obtained for 5-MTHF, 5-MDHF, the *s*-triazine degradation product, and 2-CE-5-MTHF (**6**) under most conditions as confirmed in the parity plots. In addition, no trend was observed within the residuals, and on the basis of the normalized parameter covariance matrix, none of the parameters were highly correlated to each other.

Article

J. Agric. Food Chem., Vol. 58, No. 10, 2010 **6195**

Dihydroxyacetone (0.04 mM)
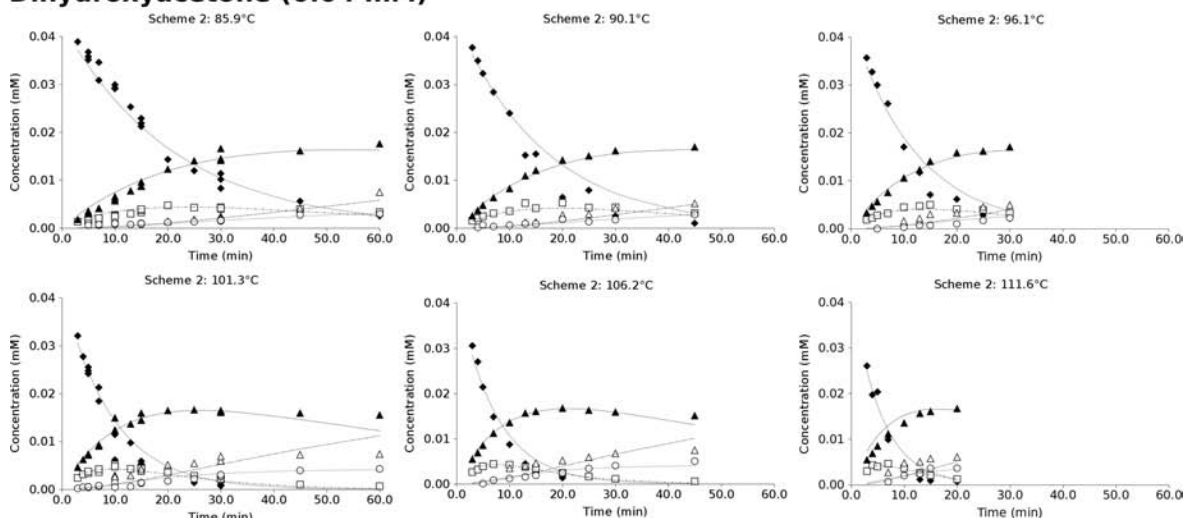
Fructose (0.04 mM)
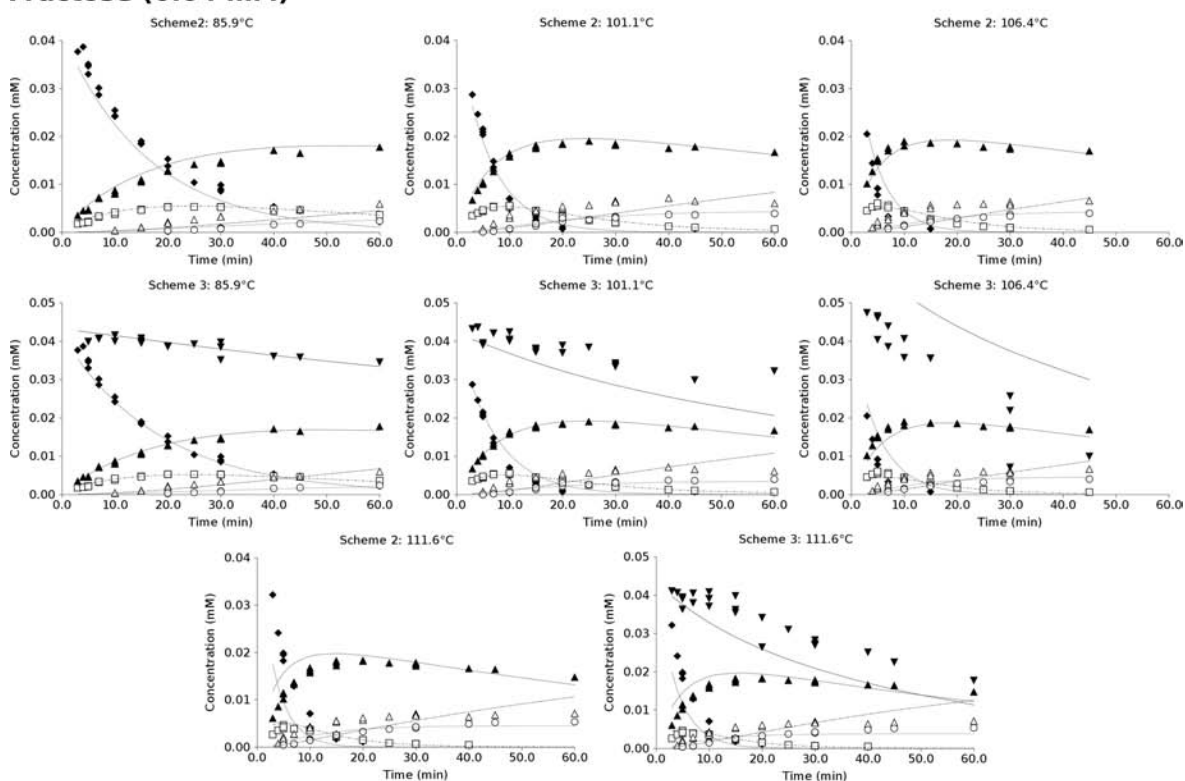
Glucose (0.04 mM)
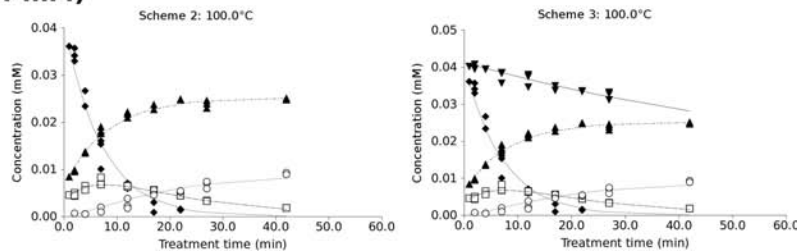
Figure 3. Experimental and predicted time course for the degradation of 5-MTHF (0.04 mM, ◆) and the formation of 5-MDHF (□), p-ABG (△), the *s*-triazine oxidation product (▲), and 2-CE-5-MTHF (○) in water heated (85–110 °C, 0–60 min) in the presence of 0.04 mM dihydroxyacetone, fructose (▼), or glucose (▼). Each experimental data point represents an independent measurement value (*n* = 1). Lines represent the predicted multiresponse model fit values using the Arrhenius equation based on kinetic reaction models excluding (**Scheme 2**) or including (**Scheme 3**) prediction of dihydroxyactone, fructose, or glucose concentrations by an apparent first-order reaction.

The estimated parameters, that is, the k_{ref} and E_a values, corresponding to the "elementary" reactions in **Scheme 2** are listed with their 95% highest posterior density (HPD) confidence interval in **Table 2**.

Table 2. Estimated k_{ref} and E_a Values for Degradation Reactions of 5-MTHF (0.04 mM) in Water in the Presence of Equimolar Amounts of Dihydroxyacetone or Fructose during Thermal Treatments (85–110 °C, 0–60 min) Based on Kinetic Reaction Models Excluding (**Scheme** 2) or Including (**Scheme** 3) Prediction of Dihydroxyactone, Fructose, or Glucose Concentrations by an Apparent First-Order Reaction[a]

| | temperature dependence (85–110 °C) | | | | |
| | dihydroxyacetone | | fructose | | glucose |
reaction	$k_{T_{ref}}{}^{b}$ ($\times 10^{-3}$ min^{-1})	E_a (kJ mol^{-1})	$k_{T_{ref}}{}^{b}$ ($\times 10^{-3}$ min^{-1})	E_a (kJ mol^{-1})	k^{c} ($\times 10^{-3}$ min^{-1})
Scheme 2					
1 → 2	17.7 ± 1.2	62.7 ± 7.1	22.8 ± 1.3	68.2 ± 6.3	35.7 ± 2.9
2 → 4	34.4 ± 5.5	75.0 ± 16.5	21.5 ± 2.8	69.5 ± 12.3	14.9 ± 3.5
1 → 4	32.5 ± 1.9	52.4 ± 6.2	50.2 ± 3.3	69.8 ± 7.1	71.5 ± 3.1
4 → 3	10.9 ± 1.4	41.3 ± 12.9	6.9 ± 1.0	32.8 ± 13.1	4.0 ± 1.1
1 → 5	27.3 ± 1.6	69.1 ± 5.9	38.4 ± 2.9	77.6 ± 7.8	47.2 ± 5.4
2 → 6	24.8 ± 2.3	61.3 ± 9.3	18.3 ± 1.2	79.5 ± 6.1	47.4 ± 2.7

| | fructose | | glucose |
reaction	$k_{T_{ref}}{}^{b}$ ($\times 10^{-3}$ min^{-1})	E_a (kJ mol^{-1})	k^{c} ($\times 10^{-3}$ min^{-1})
Scheme 3			
1 → 2	21.3 ± 1.2	68.9 ± 5.9	32.9 ± 2.5
2 → 4	29.8 ± 3.5	66.7 ± 11.2	18.3 ± 3.8
1 → 4	43.4 ± 2.7	67.8 ± 6.6	55.1 ± 3.4
4 → 3	9.9 ± 1.4	20.6 ± 12.4	0.9 ± 1.1
1 → 5	32.2 ± 2.3	77.8 ± 7.4	52.8 ± 5.3
2 → 6	437.8 ± 41.9[d]	87.0 ± 8.8	1272.6 ± 88.8[d]
7 → 8	6.6 ± 2.9	80.6 ± 39.9	7.9 ± 0.6

[a] Values are presented ± 95% HPD interval. [b] T_{ref} = 95 °C. [c] T = 100 °C. [d] k_8 ($\times 10^{-3}$ min^{-1} mM^{-1}).

In general, the reaction model underestimated the responses for p-ABG under most conditions. This lack of fit of the model pointed to the presence of an additional route of p-ABG formation that could not be quantified on the basis of the current data. Nevertheless, the goodness of fit for the total data set was satisfactory, and the model remained statistically acceptable to describe the different responses measured based on the replicate experiments. Remarkably, the current modeling results significantly point to the direct formation of 2-CE-5-MTHF from 5-MDHF by reaction with dihydroxyacetone and not to a direct reaction of the latter with 5-MTHF. Comparison with the estimated parameters obtained in the absence of dihydroxyacetone in our previous work (*12*) showed that addition of dihydroxyacetone resulted in an acceleration of the formation of 5-MDHF from 5-MTHF and also in an acceleration of the formation of p-ABG from the *s*-triazine as reflected in the estimated k_{ref} values at 95 °C. This observation could be declared by the production of hydroxyl radicals from the reaction between dissolved oxygen and the dihydroxyacetone enediol intermediate that is formed during isomerization of dihydroxyacetone to glyceraldehyde and vice versa. Such hydroxyl radical formation was shown to occur during the reaction of dihydroxyacetone with hydrogen peroxide (*21*) and was previously suggested to occur in the diradical degradation mechanism of reducing carbohydrates by oxygen (*22*). Therefore, the current observations are in line with the involvement of hydroxyl radicals in C(11)–N(12) bond cleavage of the *s*-triazine (*12*).

The fit of the kinetic model indicated that the proposed reaction model is suitable to explain the experimental data. However, it is not known whether the formation of 2-CE-5-MTHF occurs by reaction of 5-MTHF directly with dihydroxyacetone as suggested for the nonenzymatic glycation of folic acid (*15*) or whether the reaction involves degradation products from dihydroxyacetone. In this context it should be noted that methylglyoxal, which can be formed from glyceraldehyde after isomerization of dihydroxyacetone, has been shown to yield *N*(2)-[1-(carboxyethyl)] adducts upon reaction with

guanosine (*23*). To obtain a more detailed mechanistic insight into the reaction, concentrations of dihydroxyacetone and its degradation products should be determined; however, this was outside the scope of the current work and requires further investigation.

Degradation in the Presence of Fructose. The above results indicated in accordance with a previous report for folic acid that dihydroxyacetone and fructose have a paramount impact on the degradation of 5-MTHF through nonenzymatic glycation (*16*). On the basis of the previous multiresponse results, the importance of nonenzymatic glycation of 5-MTHF (0.04 mM) was therefore investigated in the presence of an equimolar amount of fructose during thermal treatments (85–110 °C, 0–60 min). Formation of 2-CE-5-MTHF was shown to occur under the investigated conditions (**Figure 3**), suggesting that some degradation products of fructose react nonenzymatically with 5-MDHF in analogy with the above observations for dihydroxyacetone. Therefore, the measured responses of 5-MTHF, 5-MDHF, p-ABG, *s*-triazine, and 2-CE-5-MTHF were simultaneously modeled by the kinetic reaction model using eqs 3–7 (**Scheme** 2) and the starting values obtained for dihydroxyacetone (**Table 2**). As depicted in **Figure 3** the model resulted in an adequate fit for most responses, whereas concentrations of p-ABG were underestimated in analogy with the above results. Comparison of the estimated parameters for fructose with the parameters obtained for dihydroxyacetone (**Table 2**) showed that estimated k_{ref} and E_a values for the corresponding "elementary" reactions did not significantly differ in the presence of dihydroxyacetone or fructose. The results hence suggest that similar reactants are involved in the presence of dihydroxyacetone and fructose. Formation of 2-CE-5-MTHF from 5-MDHF was characterized by an apparent k value of $18.3 \pm 1.2 \times 10^{-3}$ min^{-1} at T_{ref} 95 °C and an activation energy of 79.5 ± 6.1 kJ mol^{-1}. To account for the formation of dihydroxyacetone, previously postulated to be a retro-aldolization product of fructose (*15*), fructose concentrations were measured as additional responses. The latter were incorporated in the reaction model by including a cross-reaction between

Article

J. Agric. Food Chem., Vol. 58, No. 10, 2010 **6197**

fructose and 5-MDHF so that **Scheme 2** was revised to **Scheme 3**, yielding eqs **8**–**13**.

Scheme 3
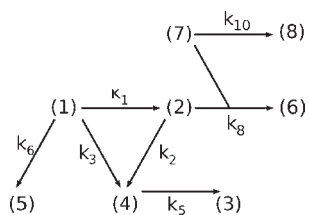
$$\frac{d[\mathbf{1}]}{dt} = -(k_1 + k_3 + k_6)[\mathbf{1}] \tag{8}$$

$$\frac{d[\mathbf{2}]}{dt} = k_1[\mathbf{1}] - k_2[\mathbf{2}] - k_8[\mathbf{2}][\mathbf{7}] \tag{9}$$

$$\frac{d[\mathbf{3}]}{dt} = k_5[\mathbf{4}] \tag{10}$$

$$\frac{d[\mathbf{4}]}{dt} = k_3[\mathbf{1}] + k_2[\mathbf{2}] - k_5[\mathbf{4}] \tag{11}$$

$$\frac{d[\mathbf{6}]}{dt} = k_8[\mathbf{2}][\mathbf{7}] \tag{12}$$

$$\frac{d[\mathbf{7}]}{dt} = -k_8[\mathbf{2}][\mathbf{7}] - k_{10}[\mathbf{7}] \tag{13}$$

The cross-reaction rate constant k_8 was postulated to account for the cumulative effect of the formation of dihydroxyacetone from fructose (**7**) and the subsequent nonenzymatic glycation reactions with 5-MDHF. It is well established that fructose undergoes several other reactions besides the formation of dihydroxyacetone upon heating in aqueous solutions producing other highly reactive low molecular weight α-hydroxycarbonyl and α-dicarbonyl compounds such as acetol and methylglyoxal, caramelization products, and carboxylic acids (*24*, *25*). Hereto, an additional reaction, characterized by k_{10}, was incorporated in the model to account for this loss of fructose and the formation of the unknown carbohydrate degradation products (**8**).

Estimated k and E_a values are shown in **Table 2** and were in accordance with the parameters that were estimated when the cross-reaction was omitted. As expected, the model adequately fitted the responses for 5-MTHF, 5-MDHF, *s*-triazine, and 2-CE-5-MTHF (**Figure 3**), whereas concentrations of p-ABG were clearly underestimated, supporting the occurrence of an additional route of formation as previously discussed. Moreover, the reaction model properly predicted fructose concentrations at 85 °C; however, it failed to render an acceptable fit for the higher temperatures. In combination with the good fit obtained for the concentrations of 2-CE-5-MTHF this observation indicates that the complex reaction network for fructose degradation at elevated temperatures cannot be modeled by a simple apparent first-order reaction.

Degradation in the Presence of Glucose. It was previously reported (*16*) that reaction of folic acid with fructose produced higher concentrations of $N(2\alpha)$-[1-(carboxyethyl)] folic acid in comparison with other reducing carbohydrates. As a 2-ketose containing a 1,3-dihydroxy-2-oxo moiety, fructose has been

postulated to be a preferential source for dihydroxyacetone compared to other monosaccharides. This hypothesis has recently been supported by the observation that 3 times more dihydroxyacetone is formed during oxidative degradation of fructose at 40 °C as compared to glucose (*24*). To investigate whether heating of 5-MTHF in the presence of glucose results in formation of 2-CE-5-MTHF, a kinetic experiment was performed at 100 °C. Measured concentrations of degradation products of 5-MTHF (0.04 mM) were tentatively modeled using **Schemes 2** and **3**, respectively, omitting and including a cross-reaction of 5-MDHF with glucose (0.04 mM). As starting values, k_{ref} values were obtained from the dihydroxyacetone data set using a reference temperature of 100 °C. Estimated k values in the presence of glucose are given in **Table 2**. As shown in **Figure 3**, the reaction models proved to result in a satisfactory fit for most responses in the presence of glucose and support the validity of the model to describe the nonenzymatic glycation of 5-MTHF. The results obtained using **Scheme 3** for glucose indicated that the degradation of this component can be described by an apparent first-order reaction model. Therefore, incorporation of a cross-reaction between glucose and 5-MDHF resulted in a better fit for the glucose concentrations as compared to the results obtained above for fructose. To clarify this discrepancy further data can be acquired on glucose and fructose degradation products to be incorporated in the current reaction model. It should be noted that this was outside the initial scope of this work and would involve extensive quantification of a lot more responses due to the known complexity of carbohydrate degradation mechanisms.

Degradation in the Presence of L-Ascorbic Acid. Addition of L-ascorbic acid to samples of 5-MTHF has previously been shown to result in significant stabilization of this vitamin in buffered solutions that undergo thermal treatments, given that a suitable amount of antioxidant is added to eliminate the dissolved oxygen (*26*). The observation that 2-CE-5-MTHF is formed by reaction of dihydroxyacetone with 5-MDHF suggested that the nonenzymatic glycation of 5-MTHF could possibly be counteracted by lowering the concentration of 5-MDHF or by preventing its formation, for example, (i) through addition of reductants (antioxidants) or (ii) by lowering the pH. Adding ascorbic acid to the unbuffered solutions in the current investigation would imply both the addition of an antioxdant and a decrease of the pH and therefore would probably decelerate or prevent formation of 5-MDHF. It should be noted, however, that L-ascorbic acid has been reported to react with guanosine, which has a similar exocyclic amino group as folates, to form advanced glycation end products at moderate temperatures (40–70 °C) in vitro (*27*). The possibility of formation of 2-CE-5-MTHF due to a reaction with L-ascorbic acid or its degradation products was, however, not taken into account previously (*26*). Hereto, degradation of 5-MTHF (0.04 mM) was screened at 100 °C (0–45 min) in the presence of an equimolar amount of fructose and L-ascorbic acid (1.13 mM). It was observed that this combination efficiently prevented the degradation of 5-MTHF under the investigated conditions because no signals for 5-MDHF, p-ABG, or 2-CE-5-MTHF were detected in the chromatograms. As shown in **Figure 4**, losses of 5-MTHF were maximally 10.4 ± 4.5%, of which oxidation to the *s*-triazine accounted for 1–3% of the total 5-MTHF loss relative to the initial folate content after 30 min of heating. Remarkably, the observed prevention of nonenzymatic glycation of folates by L-ascorbic acid is, in part, supported by the lack of detection of $N(2\alpha)$-[1-(carboxy)ethyl]folic acid in folic acid and reducing carbohydrate containing commercial products that were probably low in pH and rich in L-ascorbic acid (i.e., multivitamin juices and multivitamin sweets) reported by others (*16*); however, because folic acid is relatively stable toward
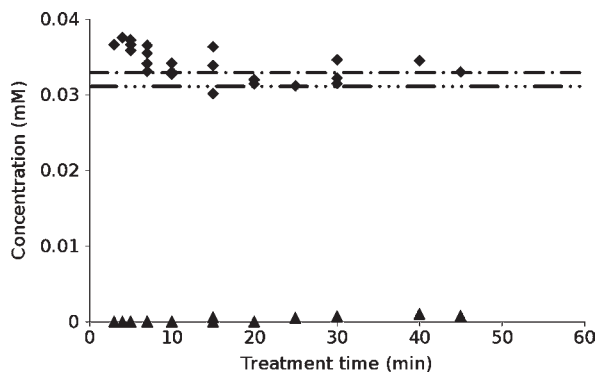
Figure 4. Time course for the degradation of 5-MTHF (◆, 0.04 mM) and the formation of its *s*-triazine oxidation product (▲) in water heated at 100 °C (0−45 min) in the presence of fructose (0.04 mM) and L-ascorbic acid (1.13 mM). Lines represent respectively 90% (− · −) and 85% (− · · · −) retention of the initial concentration of **1**. Each data point represents an independent measurement value (*n* = 1).

oxidation, the mechanism behind these observations remains unclear.

In conclusion, the stability of 5-MTHF in aqueous solution during thermal treatments (85−110 °C, 0−60 min) was shown to be decreased in the presence of dihydroxyacetone, fructose, and glucose, yielding 2-CE-5-MTHF as a nonenzymatic glycation product, characterized by LC-MS and NMR. In addition to the degradation products of 5-MTHF that were previously described (*12, 28*), concentrations of the carboxyethylated derivative were measured as an additional response in model systems heated in the presence of either dihydroxyacetone, fructose, or glucose. On the basis of model discrimination it was shown that 2-CE-5-MTHF is preferentially formed from 5-MDHF in the presence of dihydroxyacetone, indicating that the nonenzymatic glycation of this component follows the pathways summarized in **Schemes 2** and **3**. Application of these reaction models to the experimental data resulted in an adequate fit for the responses of 5-MTHF, 5-MDHF, the *s*-triazine, and 2-CE-5-MTHF in the presence of fructose and glucose. Formation of 2-CE-5-MTHF was characterized by an activation energy of 61.3 ± 9.3 and 77.6 ± 7.8 kJ mol^{-1} in the presence of, respectively, dihydroxyacetone and fructose. Addition of L-ascorbic acid (1.13 mM) to samples of 5-MTHF (0.04 mM) with fructose (0.04 mM) prior to heating at 100 °C (0−45 min) was shown to retard the formation of 5-MDHF and hence prevented the formation of 2-CE-5-MTHF under the investigated conditions.

Generally, the application of multiresponse modeling offers a good, but rarely used, way to elucidate reaction mechanisms and kinetics (on a sound statistic basis), especially in food science (*18*). For this reason we have the opinion that this publication demonstrates the value of multiresponse modeling on an appropriate example. Especially since multiresponse kinetics can be a valuable tool to assess the impact of processing techniques on nutrients where the inherent incorporation of mechanistic insights can advance the current kinetic approach for process optimization, where knowledge of the kinetic properties and activation energy of the different subreactions in the degradation process is essential. In addition, multiresponse modeling gives better results in terms of precision of parameters, which is of utmost importance for predictive modeling. This approach forces the researcher to think hard about the mechanism behind the model, thus, to integrate chemistry and physics with modeling, something believed to be essential for further progress in food science modeling.

The formation of 2-CE-5-MTHF in the investigated model systems renders it a conceivable component in foods that are similarly composed such as foods made from high-fructose corn syrup or carbohydrate-containing multivitamin beverages with low L-ascorbic acid content that undergo thermal treatments. Because knowledge of the effect of carboxyethylated folate derivatives on human metabolism is lacking, the consequences of these findings remain an open question and point to the need of further research regarding the physiological and toxicological effects of this class of derivatives. In this context, it cannot be excluded that nonenzymatic glycation of folates can occur in vivo and could be related to aging and several diseases in analogy with, for example, advanced glycation endproducts of proteins (*29*).

ABBREVIATIONS USED

5-MTHF, 5-methyl-5,6,7,8-tetrahydrofolic acid (**1**); 5-MDHF, 5-methyl-7,8-dihydrofolic acid (**2**); p-ABG: *p*-aminobenzoyl-L-glutamic acid (**3**); 2-amino-8-methyl-4,9-dioxo-7-methyl-*p*-aminobenzoylglutamate-6,7,8,9-tetrahydro-4*H*-pyrazino (1,2-a)-*s*-triazine (**4**); 2-CE-5-MTHF, *N*(2α)-[1-(carboxy)ethyl]-5-methyl-5,6,7,8-tetrahydrofolic acid (**6**).

Supporting Information Available: Additional tables and figures. This material is available free of charge via the Internet at http://pubs.acs.org.

LITERATURE CITED

(1) Eichholzer, M.; Tonz, O.; Zimmermann, R. Folic acid: a public-health challenge. *Lancet* **2006**, *367*, 1352–1361.

(2) Moat, S. J.; Lang, D.; McDowell, I. F. W.; Clarke, Z. L.; Madhavan, A. K.; Lewis, M. J.; Goodfellow, J. Folate, homocysteine, endothelial function and cardiovascular disease. *J. Nutr. Biochem.* **2004**, *15*, 64–79.

(3) Selhub, J.; Bagley, L. C.; Miller, J.; Rosenberg, I. H. B vitamins, homocysteine, and neurocognitive function in the elderly. *Am. J. Clin. Nutr.* **2000**, *71*, 614S–620S.

(4) Kim, Y. I. Folate and carcinogenesis: evidence, mechanisms, and implications. *J. Nutr. Biochem.* **1999**, *10*, 66–88.

(5) Melse-Boonstra, A.; Verhoef, P.; Konings, E. J. M.; van Dusseldorp, M.; Matser, A.; Holl- man, P. H. C.; Meyboom, S.; Kok, F. J.; West, C. E. Influence of processing on total, monoglutamate and poly-glutamate folate contents of leeks, cauliflower, and green beans. *J. Agric. Food Chem.* **2002**, *50*, 3473–3478.

(6) Verlinde, P.; Oey, I.; Hendrickx, M.; Van Loey, A. High pressure treatments induce folate polyglutamate profile changes in intact broccoli (*Brassica oleraceae* L. cv. Italica) tissue. *Food Chem.* **2008**, *111*, 220–229.

(7) Dang, J.; Arcot, J.; Shrestha, A. Folate retention in selected processed legumes. *Food Chem.* **2000**, *68*, 295–298.

(8) Indrawati; Arroqui, C.; Messagie, I.; Nguyen, M. T.; Van Loey, A.; Hendrickx, M. Comparative study on pressure and temperature stability of 5-methyltetrahydrofolic acid in model systems and in food products. *J. Agric. Food Chem.* **2004**, *52*, 485–492.

(9) Indrawati; Van Loey, A.; Hendrickx, M. Pressure and temperature stability of 5-methyltetrahydrofolic acid: a kinetic study. *J. Agric. Food Chem.* **2005**, *53*, 3081–3087.

(10) Stea, T. H.; Johansson, M. S.; Jagerstad, M.; Frolich, W. Retention of folates in cooked, stored and reheated peas, broccoli and potatoes for use in modern large-scale service systems. *Food Chem.* **2006**, *101*, 1095–1107.

(11) Vahteristo, L. T.; Lehikoinen, K. E.; Ollilainen, V.; Koivistoinen, P. E.; Varo, P. Oven-baking and frozen storage affect folate vitamer retention. *LWT−Food Sci. Technol.* **1998**, *31*, 329–333.

(12) Verlinde, P.; Oey, I.; Deborggraeve, W.; Hendrickx, M.; Van Loey, A. Mechanism and related kinetics of 5-methyltetrahydrofolic acid degradation during combined high hydrostatic pressure-thermal treatments. *J. Agric. Food Chem.* **2009**, *57*, 6803–6814.

(13) Scott, J.; Rebeille, F.; Fletcher, J. Folic acid and folates: the feasibility for nutritional enhancement in plant foods. *J. Sci. Food Agric.* **2000**, *80*, 795–824.

(14) McKillop, D. J.; Pentieva, K.; Daly, D.; McPartlin, J. M.; Hughes., J.; Strain, J. J.; Scott, J. M.; McNulty, H. The effect of different cooking methods on folate retention in various foods that are amongst the major contributors to folate intake in the UK diet. *Br. J. Nutr.* **2002**, *88*, 681–688.

(15) Schneider, M.; Klotzsche, M.; Werzinger, C.; Hegele, J.; Waibel, R.; Pischetsrieder, M. Reaction of folic acid with reducing sugars and sugar degradation products. *J. Agric. Food Chem.* **2002**, *50*, 1647–1651.

(16) Rychlik, M.; Mayr, A. Quantitation of *N*2-[1-(1-carboxy)ethyl]folic acid, a nonenzymatic glycation product of folic acid, in fortified foods and model cookies by a stable isotope dilution assay. *J. Agric. Food Chem.* **2005**, *53*, 5116–5124.

(17) Konings, E. J.; Roomans, H. H.; Dorant, E.; Goldbohm, R. A.; Saris, W. H.; van den Brandt, P. A. Folate intake of the Dutch population according to newly established liquid chromatography data for foods. *Am. J. Clin. Nutr.* **2001**, *73*, 765–776.

(18) van Boekel, M. A. J. S. *Kinetic Modeling of Reactions in Foods*; CRC Press Taylor and Francis Group: Boca Raton, FL, 2009.

(19) Stewart, W. E.; Shon, Y.; Box, G. E. P. Discrimination and goodness of fit of multiresponse mechanistic models. *AIChE J.* **1998**, *44*, 1404–1412.

(20) Poe, M.; Hensens, O. D.; Hoogsteen, K. 5-Methyl-5,6,7,8-tetrahydrofolic acid. Conformation of the tetrahydropyrazine ring. *J. Biol. Chem.* **1979**, *254*, 10881–10884.

(21) Maksimovic, V.; Mojovic, M.; Neumann, G.; Vucinic, Z. Nonenzymatic reaction of dihydroxyacetone with hydrogen peroxide enhanced via a Fenton reaction. *Ann. N.Y. Acad. Sci.* **2005**, *1048*, 461–465.

(22) Isbell, H. S. A diradical mechanism for the degradation of reducing sugars by oxygen. *Carbohydr. Res.* **1976**, *49*, C1–C4.

(23) Frischmann, M.; Bidmon, C.; Angerer, J.; Pischetsrieder, M. Identification of DNA adducts of methylglyoxal. *Chem. Res. Toxicol.* **2005**, *18*, 1586–1592.

(24) Novotny, O.; Cejpek, K.; Velisek, J. Formation of α-hydroxycarbonyl and α-dicarbonyl compounds during degradation of monosaccharides. *Czech J. Food Sci.* **2007**, *25*, 119–130.

(25) Novotny, O.; Cejpek, K.; Velisek, J. Formation of carboxylic acids during degradation of monosaccharides. *Czech J. Food Sci.* **2008**, *26*, 117–131.

(26) Oey, I.; Verlinde, P.; Hendrickx, M.; Van Loey, A. Temperature and pressure stability of L-ascorbic acid and/or [6S]5-methyletrahydrofolic acid: a kinetic study. *Eur. Food Res. Technol.* **2006**, *223*, 71–77.

(27) Seidel, W.; Pischetsrieder, M. Reaction of guanosine with glucose under oxidative conditions. *Bioorg. Med. Chem. Lett.* **1998**, *8*, 2017–2022.

(28) Whiteley, J. M.; Russell, A. Structural reassignment of the peroxide oxidation product of 5-methyl-5,6,7,8-tetrahydrofolate. *Biochem. Biophys. Res. Commun.* **1981**, *101*, 1259–1265.

(29) Gasser, A.; Forbes, J. M. Advanced glycation: implications in tissue damage and disease. *Protein Pept. Lett.* **2008**, *15*, 385–391.